HHS Public Access

Author manuscript

Muscle Nerve. Author manuscript; available in PMC 2022 April 01.

Published in final edited form as:

Muscle Nerve. 2021 April ; 63(4): 553–562. doi:10.1002/mus.27174.

Quantitative muscle MRI as a sensitive marker of early muscle pathology in myotonic dystrophy type 1

Ellen van der Plas, PhD[1], **Laurie Gutmann, MD**[2,3], **Dan Thedens, PhD**[4], **Richard K. Shields, PhD**[5], **Kathleen Langbehn, BA**[1], **Zhihui Guo, PhD**[6], **Milan Sonka, PhD**[6], **Peggy Nopoulos, MD**[1]

[1]Department of Psychiatry, University of Iowa Hospital & Clinics, Iowa City, IA, USA

[2]Department of Neurology, University of Iowa Hospital & Clinics, Iowa City, IA, USA

[3]Department of Neurology, Indiana University School of Medicine, Indianapolis, IN, USA

[4]Department of Radiology, University of Iowa Hospital & Clinics, Iowa City, IA, USA

[5]Department of Physical Therapy and Rehabilitation Science, University of Iowa Hospital & Clinics, Iowa City, IA, USA

[6]Iowa Institute for Biomedical Imaging, University of Iowa, Iowa City, IA, USA

Abstract

Introduction—The utility of muscle MRI as a marker of muscle pathology and disease progression in adult-onset myotonic dystrophy type 1 (DM1) was evaluated.

Methods—This prospective, longitudinal study included 67 observations from 36 DM1 patients (50% female), and 92 observations from 49 healthy adults (49% female). Lower-leg 3T magnetic resonance images (MRI) were acquired. Volume and fat fraction (FF) were estimated using a 3-point Dixon method, and T2-relaxometry was determined using a multi-echo spin-echo sequence. Muscles were segmented automatically. Mixed linear models were conducted to determine group differences across muscles and image modality, accounting for age, sex and repeated observations. Differences in rate of change in volume, T2-relaxometry and FF were also determined with mixed linear regression that included a group by elapsed time interaction.

Results—Compared with healthy adults, DM1 patients exhibited reduced volume of the tibialis anterior, soleus, and gastrocnemius (all, $p<0.05$). T2-relaxometry and FF were increased across all calf muscles in DM1 compared to controls. (all, $p<0.01$). Signs of muscle pathology, including reduced volume, and increased T2-relaxometry and FF were already noted in DM1 patients who did not exhibit clinical motor symptoms of DM1. As a group, DM1 patients exhibited a more rapid change than did controls in tibialis posterior (TP) volume ($p=0.05$) and gastrocnemius (GAS) T2-relaxometry ($p=0.03$) and FF ($p=0.06$)

Corresponding author Ellen van der Plas, W280 GH, Department of Psychiatry, University of Iowa Hospital & Clinics, Iowa City, IA 52242; 319 353 8544; ellen-vanderplas@uiowa.edu.

Discussion—Muscle MRI renders sensitive, early markers of muscle pathology and disease progression in DM1. T2 relaxometry may be particularly sensitive to early muscle changes related to DM1.

Keywords

Magnetic Resonance Imaging (MRI); Myotonic Dystrophy (DM1); Muscle segmentation; T2-relaxometry Fat fraction (FF)

Introduction

Myotonic dystrophy type 1 (DM1) is an autosomal dominant, trinucleotide-repeat disorder caused by a CTG repeat expansion on the myotonic dystrophy protein kinase gene (*DMPK*).[1] The disorder is primarily defined by progressive muscle wasting, weakness, and myotonia.[2] With potential therapies on the horizon,[3,4] there is an increased urgency for identifying reliable and reproducible markers of disease progression. Attempts to develop sensitive biomarkers include muscle biopsies,[5] extracellular RNA markers in urine,[6] and muscle strength[7] and neurophysiological testing.[8] However, with these approaches do cannot assess the structure of multiple individual muscles simultaneously, which is an important limitation in the context of prior findings showing that each skeletal muscle may be affected differently by DM1.[9] Furthermore, the amount of fat infiltration and muscle volume cannot be quantified with these methods.

Magnetic resonance imaging (MRI) offers a quantitative, non-invasive alternative for evaluating a variety of muscles and pathophysiological mechanisms, including muscle atrophy (volume), proxy for degree of edema and inflammation (T2-relaxometry), and fatty infiltration (3-point Dixon fat fraction).[10] Work in Duchenne muscular dystrophy showed that muscle MRI can be used to monitor change over time, and produces reliable and reproducible results in a multisite setting.[11] Studies in DM1[12] and Becker muscular dystrophy[13] demonstrated that muscle volume, fat fraction (FF), and T2-relaxometry are promising biomarkers for assessing disease state of skeletal muscles. However, manual tracing for delineating individual muscles[12,13] is arduous and time consuming, limiting its utility in large research settings. Semi-automated muscle segmentation methods for use in DM1 patients have recently been developed.[10,14]. One group used image intensity thresholds to delineate lower leg muscles, but did not differentiate between individual muscles.[14] Others used a method that required up to ten slices of manual tracing per participant.[10] Automated segmentation of individual muscle compartments is necessary to improve the efficiency and utility of muscle MRI as a marker of muscle pathology. It is also important to evaluate if muscle MRI is useful for detecting disease pathology before the onset of overt symptoms,[15] which would make MRI a potentially useful tool for trials on disease prevention. Finally, it needs to be determined if MRI is sensitive to disease progression by evaluating change in muscle pathology over time.

Our group recently developed an automated muscle segmentation approach that was demonstrated to be as accurate as manual tracings.[16] The first goal of the present study was to apply the automated muscle segmentation approach, and determine the utility of

lower-leg muscle MRI as a marker of DM1-related pathology across lower leg muscles. Second, we evaluated if muscle MRI detected early muscle pathology in individuals who had inherited the CTG expansion, but had not yet manifested clinical motor symptoms or signs (i.e., PreDM1). Third, we compared rate of change in volume, T2-relaxometry and FF between DM1 patients and healthy adults.

Methods

Participants

The Iowa Brain and Muscle study was targeted to patients with adult-onset DM1. The current analysis evaluated individuals with a clinical diagnosis of DM1, and individuals with a family history of DM1 (referred to as 'at-risk), who were recruited through The Myotonic Dystrophy Foundation and word of mouth. Individuals who were considered 'at-risk' were offspring or siblings of participants with DM1. Unaffected participants were primarily recruited from the local community via advertisements. Recruitment for the study took place between March 2016 and February 2020. Participants were assessed at a maximum of 3 occasions that were approximately 1 year apart.

Individuals were included in this study if they met the following criteria: (1) diagnosis of adult-onset DM1, which was operationalized as diagnosis after the age of 18; or 'at-risk' individuals with family history of DM1, but who had not undergone genetic testing themselves; (2) between 18 and 70 years old at evaluation; (3) no MRI contraindications; and (4) no history of major head trauma requiring a hospital stay. Note that the latter criterion was implemented as part of a companion neuroimaging study.[17] In addition to the criteria noted above, the comparison group of healthy adult individuals were required to have CTG repeats in the normal range, and be without a history of substance abuse, psychiatric disease, or major medical disease, including heart disease, sleep disorder, vascular disease, uncontrolled hypertension, cancer, diabetes mellitus, lung disease, autoimmune conditions, and neuromuscular disease (and specifically DM1/DM2).

All participants underwent genetic testing for research purposes only. At-risk individuals who were determined to have CTG repeat length ≥ 50 were included in the DM1 group. The remainder had CTG repeat length in the non-disease associated range and were included in the unaffected group (Supplementary Figure 1).

Motor impairment was assessed with the Muscular Impairment Rating Scale (MIRS), which is a clinical evaluation of motor impairment based on an ordinal scale ranging from 1 (asymptomatic) to 5 (severe proximal weakness).[18] A neurologist (LG) used MIRS to determine clinical motor signs and symptoms of DM1. For the purposes of the present study, individuals with a score of 1 were classified as PreDM1 and individuals with MIRS >1 were classified as manifest DM1.

Research staff, clinicians, and scientists involved in this study were blind to the genetic status of at-risk individuals. All data were deidentified and all participants consented to non-disclosure of genetic results. All participants gave written, informed consent prior to

enrolling in the protocol in accordance with the Declaration of Helsinki. The study was approved by the University of Iowa Institutional Review Board.

Estimated progenitor allele length (ePAL)

Genotyping of CTG repeat was completed by SP-PCR.[19] For each patient, four reactions were completed, each using 300pg genomic DNA template derived from blood leukocytes. CTG repeat length was estimated by comparison against DNA fragments of known length and molecular weight markers, using CLIQS software (TotalLabs UK Ltd.). The lower boundary of the expanded molecules in SP-PCR was used to estimate ePAL.[20]

MRI acquisition—Images of the calf were acquired on a GE MR750 Discovery 3T scanner using an eight-channel anterior/posterior body array coil with bilateral coverage. FF estimates were derived from a 3-point Dixon gradient echo sequence[21] with echo times of 3.45 ms, 4.60 ms, and 5.75 ms. Each echo time was taken in a separate acquisition with common parameters TR = 150ms, field of view 36 cm, resolution 0.7mm x 1.4mm, slice thickness 7mm, bandwidth 244 Hz/pixel, scan time 2m36s for each of the three echoes. FF was defined as the signal arising from fat protons divided by the sum of the signals from fat and water protons:

$$FF = \frac{fat}{fat + \text{water}} * 100$$

The TE = 3.45 ms was also used for image segmentation of the muscle groups to ensure accurate registration.

T2 relaxation maps derived from a multi-echo (initial TE 11 ms), multi-slice spin echo sequence with 16 echoes spaced by 10.8 ms with a TR of 1500ms and bandwidth 164 Hz/pixel. Slice crushers were applied around each refocusing pulse to mitigate the effects from stimulated echoes. Acquired in-plane resolution was 1.0mm x 2.0mm with 0.7mm slices and identical coverage to that of the 3-point Dixon scans. The total scan time was 7m21s. T2 maps were generated from multi-echo data using a non-linear least-squares monoexponential curve fitting algorithm. T2 and Dixon sequences were acquired in two passes (even and odd slices, respectively). The tibial plateau was used as the superior landmark and 210mm long coverage of calf muscle tissue was imaged in 30 contiguous 7mm-thick MR slices.

Calf muscle segmentation—Five major muscle compartments – including tibialis anterior (TA), tibialis posterior (TP), peroneus longus (PL), soleus (SOL), gastrocnemius (GAS) (Supplementary Figure 2) – were automatically and simultaneously segmented from volumetric MR images using a convolutional neural network approach that was trained using manually-traced examples. Our segmentation approach, called FilterNet, has been demonstrated to yield highly accurate volumetric segmentation, with mean DICE coefficients ranging between 88% and 91%.[16] From the available 3D MR dataset, the single most superior and single most inferior slices were excluded from analysis due to the presence of bone-related artifacts. While the absolute axial length of the analyzed calf muscles was fixed at 196 mm (28 analyzed slices x 7 mm), the inferior endpoints of the anatomic coverage may have varied slightly across participants due to their unequal tibial

length. In locations where the automated segmentation did not identify the muscle surfaces with sufficient accuracy, segmentation was improved by slice-by-slice editing by trained individuals.

Statistical analysis

Demographic characteristics of DM1 patients and unaffected individuals were summarized using descriptive statistics. Clinical characteristics in DM1 patients were also described, including ePAL and MIRS. To account for large range differences across image modalities and muscle compartments, each outcome measure was scaled by subtracting the grand mean and dividing by the SD for that measure.

Group differences in muscle volume, T2-relaxometry and FF were determined using mixed linear regression for each muscle (TA, TP, PL, SOL, GAS; left/right combined), across imaging modality (volume, T2-relaxometry, and FF). The models included group, age and sex as predictor variables, and random effects for family relations and participant. The false discovery rate (FDR) was used to account for multiple comparisons.[22] Pairwise comparisons were performed to determine which group(s) were driving the main effect. To convey differences between groups on the plots, model-generated estimated marginal means (EMM) were centered around the EMM of unaffected individuals.

To evaluate potential group differences in change in muscles across image modalities, mixed linear regression models were conducted with the change score as the dependent variable (e.g., change in gastrocnemius volume from baseline visit), and group*elapsed time as the predictor variable. Age at baseline and sex were also included as predictor variables, in addition to random effects for family and participant. Individuals with PreDM1 and DM1 were collapsed into one group for these analyses, because the PreDM1 group was considered too small for conducting meaningful analyses on interaction effects. The effect of interest, group*elapsed time provides an estimate of the difference in rate of change between groups in 1 year.

Associations between ePAL and imaging outcomes were explored within the DM1 sample only, using mixed linear models that included ePAL, age, sex and random effects for participant and family as predictor variables. All analyses were performed in R version 3.5.0 (https://www.R-project.org).

Results

Study sample

Table 1 summarizes demographic and clinical characteristics of the sample observations. The final sample included 92 observations from healthy adults (49 unique individuals; 26 females [53%]), 16 observations from individuals with PreDM1 (10 unique individuals; 5 females [50%]), and 51 observations from individuals with manifest DM1 (26 unique individuals; 16 females 62%]). For those with repeated visits, average elapsed time between visits was 1.2 years (SD=0.33).

On average, individuals were 44.4 years old at evaluation (SD=12.77 years). The preDM1 group was slightly older than the manifest DM1 group ($t_{(73.9)}=-2.69$, $p<0.01$); however, none of the other comparisons were statistically significant (all, $p>0.13$). The distribution of males and females was equal across groups, $X_{((2)}^2=0.12$, p=0.549. The Wilcoxon Rank Test showed that the PreDM1 groups had significantly fewer repeats than did the manifest DM1 group, W=3135, $p<0.00001$. Finally, height and weight did not significantly differ between groups ($F_{(2, 87.7)}=0.37$, $p=0.69$ and $F_{(2, 90.2)}=2.14$, $p=0.12$, respectively).

Group differences across image modality and muscle compartment

Figure 1 shows representative examples of each image modality from three similar-aged males drawn from each group. Figure 2 depicts the age- and sex adjusted estimated marginal means (EMM) for each group across image modalities and muscles. Statistics for the main effects of group, age, and sex are shown in Supplementary Table 2. Detailed statistics for the pairwise comparisons across groups are presented in Table 2. For completeness, non-standardized values are presented in Supplementary Table 3.

Volume

Group was a significant predictor of TA, SOL, and GAS (See Supplementary Table 2 for details). Pairwise comparisons for TA volume showed that individuals with PreDM1 had significantly reduced volume relative to controls. Likewise, the DM1 group exhibited reduced TA volume compared with controls. However, there was no significant difference between PreDM1 and DM1 (Supplementary Table 1; Figure 2).

For SOL volume, pairwise comparisons showed no difference between controls and PreDM1. Individuals with DM1 had reduced SOL volume relative to controls (Supplementary Table 1, Figure 2). There was no difference in SOL volume between the PreDM1 and DM1 groups.

Pairwise comparison of the GAS volume showed that individuals with PreDM1 had reduced volume relative to controls. Likewise, the DM1 group exhibited reduced GAS volume compared with controls, but there was no difference between PreDM1 and DM1 (Supplementary Table 1; Figure 2).

T2 relaxation

The main effect of group was for T2 relaxometry of the TA, TP, SOL, GAS, and PL (Supplementary Table 2). The group effect for TA was driven by the difference between DM1 and controls (See Supplementary Table 1 for all pairwise comparisons), where the DM1 group exhibited increased T2 relaxation relative to controls.

Pairwise comparisons of T2 relaxometry of the TP showed that the PreDM1 group had elevated T2 compared with controls. The DM1 group showed similarly elevated T2 relaxometry in TP compared with controls, but there was no difference between PreDM1 and DM1. A similar pattern of differences was observed for SOL, GAS, and PL T2-relaxometry (Supplementary Table 1; Figure 2).

Fat fraction

The group predictor was significant for FF of TP, SOL, GAS, and PL (Supplementary Table 2). Pairwise comparison for TP showed that the PreDM1 group had elevated FF compared with controls. The DM1 group also exhibited elevated TP FF relative to controls. Additionally, the PreDM1 group showed higher FF than the DM1 group for this muscle.

For SOL FF, differences were observed between controls and PreDM1, controls and DM1, but not between PreDM1 and DM1. Both the PreDM1 group and the DM1 group exhibited elevated SOL FF relative to controls. The same pattern of differences was observed for GAS FF (Figure 2; Supplementary Table 1).

The group effect for PL was driven by an elevation in FF in PreDM1 compared with controls and PreDM1 (see Supplementary Table 1 for all pairwise comparisons).

Change over elapsed time—The analyses included 143 observations, 60 of which came from individuals with DM1 (PreDM1 and DM1 collapsed into one group), and 83 came from healthy adults. The group*elapsed time interaction was significant for TP volume (Table 2; Figure 3), where DM1 patients exhibited a decrease in volume, while controls remained stable. A group*elapsed time interaction was also observed for GAS T2-relaxometry and GAS FF, where the DM1 group exhibited an increase while the controls remained relatively stable (Table 2; Figure 3). See Table 3 for interaction statistics across all dependent variables.

ePAL—Models evaluating associations between ePAL and muscle MRI were limited to DM1 (preDM1 and manifest DM1 combined). Summary statistics for associations between ePAL and image modality are listed in Table 3. Increased ePAL was associated with decreased volume of TA, and increased T2-relaxometry of GAS (Table 3; Figure 4).

Discussion

Compared with healthy adults, individuals with DM1 exhibited reduced lower leg muscle volume (atrophy), increased T2-relaxometry (proxy for edema), and higher FF. Indices of pathology were noted across muscle compartments, and individuals with preDM1 exhibited muscle pathology as detected with MRI, even though they had not yet manifested clinical signs and symptoms of DM1. Examination of change in muscle pathology showed that individuals with DM1 exhibited increased GAS T2-relaxometry and FF relative to healthy adults. Finally, ePAL was associated with GAS T2-relaxometry and with TA volume. Collectively, our results show that muscle MRI with automated muscle segmentation is a sensitive marker of muscle pathology and disease progression in DM1.

Detection of changes early in the course of disease is of vital importance in the context of a potential biomarker. The majority of patients in the present sample were relatively mildly affected: of those with manifest symptoms or signs, 60% were categorized as having minimal muscle impairment (MIRS=2). Moreover, a subset of patients in the study was classified as having no motor signs or symptoms of DM1. When compared to healthy adults, there are clear differences in muscle MRI findings in individuals classified as

PreDM1, specifically with decreased volume and increased fatty infiltration.. Heskamp and colleagues[12] suggested that edema-associated processes may occur prior to fat infiltration. Cross-sectional comparisons between groups in the present study showed that both putative edema and fat infiltration was already evident in pre-symptomatic DM1 patients. While T2-relaxation is generally considered a measure of edema,[12] it is also influenced by fatty infiltration. As fat suppression was not implemented for the T2-relaxometry acquisition, we cannot make strong inferences about the pathological underpinnings of increased T2-relaxometry.

Analyses evaluating change in muscle MRI showed that compared with healthy adults, individuals with DM1 exhibited an accelerated rate of change in TP volume, and T2-relaxation time and FF in GAS. Groups diverged in rate of change after 1 year, particularly for GAS T2-relaxometry. These results are vital for clinical trials, as the efficacy of a drug in slowing disease progression may reliably be assessed after a relatively short period of time. With larger samples that also include more severely affected patients, a more robust difference in rate of change may be observed.

Until recently, manual[12] and semi-automated[10,14] segmentation of muscles were the only available techniques for delineation of calf muscles. Severe muscle pathology associated with DM1 had thus far prevented the use of automated muscle segmentation.[10] Our segmentation tool showed excellent agreement with manual tracings.[16] Automated labeling enhances efficiency of muscle MRI. This feature not only increases feasibility of the use of muscle MRI in the clinic,[16] it also benefits multi-site research initiatives that include large numbers of patients. Differences in volume, T2-relaxometry, and FF between unaffected individuals and manifest DM1 patients were generally in line with previous work using manual muscle segmentation.[12,15] However, while Heskamp and colleagues[12] observed significant associations between increased lower leg muscle FF and ePAL, we observed more robust associations between ePAL and T2-relaxometry. These seemingly discrepant findings may be due to differences in sample composition between the studies. Nearly half of the sample reported in Heskamp and colleagues[12] included patients with infantile- or juvenile-onset DM1, whereas the present study was composed of adult-onset DM1 patients only. Age of onset is associated with CTG repeat length,[23,24] and mean ePAL of the current sample of manifest DM1 patients was 1.6 times lower than that of the sample reported in Heskamp et al[12]. Additionally, total T2-relaxation in the present study could have been influenced by FF. It is possible that the reported association between ePAL and T2-relaxometry could at least in part reflect some FF involvement. It will be important to examine muscle MRI across DM1 phenotypes to determine potential differences in muscle pathology. This notion is particularly important in the context of automated muscle segmentation, as it is possible that the severity of muscle pathology in childhood- and juvenile-onset DM1 precludes use of a fully automated approach.

This study is not without limitations. For instance, overt and obvious motor symptoms in manifest individuals may have precluded blinding of research staff interacting with participants. The large number of comparisons increased potential of Type 1 errors. We reported FDR to address this concern. The observed group differences typically remained significant after FDR correction; however, the analyses evaluating change over time and

associations with ePAL should be interpreted with caution. Replication in a larger sample of DM1 patients is warranted.

Additionally, the sample was limited to adult-onset DM1 only, and individuals in the sample were relatively mildly affected. These features limit generalizability of the results. Moreover, severity of disease can affect accuracy of automated muscle segmentation. While most automated segmentations in the present study needed little to no editing (>90%), a small percentage required more extensive manual intervention, usually due to severely diseased muscles. Nonetheless, the combination of automated segmentation with expert editing resulted in an efficient approach of quantitative volumetric analysis of the entire set of five calf-muscle compartments.

Another consideration is the limited amount of knowledge on the sensitivity of MRI-based measures in detecting treatment-induced slowing of disease progression. Relatedly, elevations in certain image modalities such as T2-relaxometry may represent a variety of pathophysiological processes, including increased edema and fatty infiltration. Other magnetization transfer effects may also have introduced bias in the T2 measurements, which could become an issue in studies that include multiple MRI systems.[25] It is therefore important to continue to explore potential endpoints for clinical trials aimed at reducing disease burden of DM1.

Established biomarkers for potential clinical trials in DM1 are especially important as the field moves forward with potential gene therapies and gene-modifying therapies in this and other triplet-repeat disorders. This study provides strong evidence for a difference in MRI modalities that can be found in DM1 patients compared to unaffected adults, including in those who have not yet developed clinical signs or symptoms of the disease. MRI is non-invasive, sensitive to disease progression, and provides insight into early changes related to muscle pathology, making it a promising tool for clinical trials. Moreover, the implementation of automated muscle segmentation methods will improve efficiency of muscle MRI in a large-scale setting.

Supplementary Material

Refer to Web version on PubMed Central for supplementary material.

Acknowledgements

This study was funded by the National Institute of Neurological Disorders and Stroke. None of the authors has any conflict of interest to disclose. We confirm that we have read the Journal’s position on issues involved in ethical publication and affirm that this report is consistent with those guidelines

Abbreviations

DM1	myotonic dystrophy type 1
MRI	magnetic resonance imaging
FF	fat fraction

DMPK	myotonic dystrophy protein kinase gene
TA	tibialis anterior
TP	tibialis posterior
PL	peroneus longus
SOL	soleus
GAS	gastrocnemius
MIRS	Muscular Impairment Rating Scale
EMM	estimated marginal means
FDR	false discovery rate
ePAL	estimate the progenitor allele length

References

1. Meola G, Cardani R. Myotonic dystrophies: An update on clinical aspects, genetic, pathology, and molecular pathomechanisms. Biochimica et Biophysica Acta – Molecular Basis of Disease2015; 1852:594–606. Published online: 2015. DOI: 10.1016/j.bbadis.2014.05.019.
2. Bird T. Myotonic Dystrophy Type 1. GeneReviews®. https://www.ncbi.nlm.nih.gov/books/NBK1165/. Published1999.
3. Thornton CA, Wang E, Carrell EM. Myotonic dystrophy: approach to therapy. Current Opinion in Genetics & Development2017; 44:135–140. Published online: June 2017. DOI: 10.1016/j.gde.2017.03.007. [PubMed: 28376341]
4. Babačić H, Mehta A, Merkel O, Schoser B. CRISPR-cas gene-editing as plausible treatment of neuromuscular and nucleotide-repeat-expansion diseases: A systematic review. PLoS ONE2019; 14:1–32. Published online: 2019. DOI: 10.1371/journal.pone.0212198.
5. Nakamori M, Sobczak K, Puwanant A, Welle S, Eichinger K, Pandya S, et al.Splicing biomarkers of disease severity in myotonic dystrophy. Annals of Neurology2013; 74:862–872. Published online: December 2013. DOI: 10.1002/ana.23992. [PubMed: 23929620]
6. Antoury L, Hu N, Balaj L, Das S, Georghiou S, Darras B, et al.Analysis of extracellular mRNA in human urine reveals splice variant biomarkers of muscular dystrophies. Nature Communications2018; 9:1–16. Published online: 2018. DOI: 10.1038/s41467-018-06206-0.
7. Moxley RT, Logigian EL, Martens WB, Annis CL, Pandya S, Moxley IV RT, et al.Computerized hand grip myometry reliably measures myotonia and muscle strength in myotonic dystrophy (DM1). Muscle and Nerve2007; 36:320–328. Published online: 2007. DOI: 10.1002/mus.20822. [PubMed: 17587223]
8. Shields RK, Lee J, Buelow A, Petrie M, Dudley-Javoroski S, Cross S, et al.Myotonic dystrophy type 1 alters muscle twitch properties, spinal reflexes, and perturbation-induced trans-cortical reflexes. Muscle and Nerve2020; 61:205–212. Published online: 2020. DOI: 10.1002/mus.26767. [PubMed: 31773755]
9. Kornblum C, Lutterbey G, Bogdanow M, Kesper K, Schild H, Schröder R, et al.Distinct neuromuscular phenotypes in myotonic dystrophy types 1 and 2: A whole body highfield MRI study. Journal of Neurology2006; 253:753–761. Published online: 2006. DOI: 10.1007/s00415-006-0111-5. [PubMed: 16511650]
10. Ogier AC, Heskamp L, Michel CP, Fouré A, Bellemare ME, Le Troter A, et al.A novel segmentation framework dedicated to the follow-up of fat infiltration in individual muscles of patients with neuromuscular disorders. Magnetic Resonance in Medicine2020; 83:1825–1836. Published online: 2020. DOI: 10.1002/mrm.28030. [PubMed: 31677312]

11. Forbes SC, Arora H, Willcocks RJ, Triplett WT, Rooney WD, Barnard AM, et al.Upper and Lower Extremities in Duchenne Muscular Dystrophy Evaluated with Quantitative MRI and Proton MR Spectroscopy in a Multicenter Cohort. Radiology2020; 295:616–625. Published online: June 2020. DOI: 10.1148/radiol.2020192210. [PubMed: 32286193]
12. Heskamp L, Van Nimwegen M, Ploegmakers MJ, Bassez G, Deux JF, Cumming SA, et al.Lower extremity muscle pathology in myotonic dystrophy type 1 assessed by quantitative MRI. Neurology2019; 92:E2803–E2814. Published online: 2019. DOI: 10.1212/WNL.0000000000007648. [PubMed: 31118244]
13. Maggi L, Moscatelli M, Frangiamore R, Mazzi F, Verri M, De Luca A, et al.Quantitative Muscle MRI Protocol as Possible Biomarker in Becker Muscular Dystrophy. Clinical Neuroradiology2020. Published online: 2020. DOI: 10.1007/s00062-019-00875-0.
14. Müller M, Dohrn MF, Romanzetti S, Gadermayr M, Reetz K, Krämer NA, et al.Semi-automated volumetry of MRI serves as a biomarker in neuromuscular patients. Muscle and Nerve2020; 61:600–607. Published online: 2020. DOI: 10.1002/mus.26827. [PubMed: 32022288]
15. Peric S, Maksimovic R, Banko B, Durdic M, Bjelica B, Bozovic I, et al.Magnetic resonance imaging of leg muscles in patients with myotonic dystrophies. Journal of Neurology2017; 264:1899–1908. Published online: 2017. DOI: 10.1007/s00415-017-8574-0. [PubMed: 28756605]
16. Guo Z, Zhang H, Chen Z, van der Plas E, Gutmann L, Thedens D, et al.FilterNet: A Neighborhood Relationship Enhanced Fully Convolutional Network for Calf Muscle Compartment Segmentation. arXiv June 2020. Published online: June 21, 2020.
17. van der Plas E, Hamilton MJ, Miller JN, Koscik TR, Long JD, Cumming S, et al.Brain Structural Features of Myotonic Dystrophy Type 1 and their Relationship with Ctg Repeats. Journal of neuromuscular diseases July 2019. Published online: July 8, 2019. DOI: 10.3233/JND-190397.
18. Mathieu J, Boivin H, Meunier D, Gaudreault M, Bégin P. Assessment of a disease-specific muscular impairment rating scale in myotonic dystrophy. Neurology2001; 56:336–340. Published online: 2001. DOI: 10.1212/WNL.56.3.336. [PubMed: 11171898]
19. Gomes-Pereira M, Bidichandani SI, Monckton DG. Analysis of Unstable Triplet Repeats Using Small-Pool Polymerase Chain Reaction. In: Trinucleotide Repeat Protocols. Humana Press: New Jersey; 2004. p. 061–076http://link.springer.com/10.1385/1-59259-804-8:061.
20. Monckton DG, Wong LJC, Ashizawa T, Caskey CT. Somatic mosaicism, germline expansions, germline reversions and intergenerational reductions in myotonic dystrophy males: small pool PCR analyses. Human Molecular Genetics1995; 4:1–8. Published online: 1995. DOI: 10.1093/hmg/4.1.1. [PubMed: 7711720]
21. Glover GH, Schneider E. Three-point dixon technique for true water/fat decomposition with B0 inhomogeneity correction. Magnetic Resonance in Medicine1991; 18:371–383. Published online: 1991. DOI: 10.1002/mrm.1910180211. [PubMed: 2046518]
22. Benjamini Y, Hochberg Y. Controlling the false discovery rate: a practical and powerful approach to multiple testing. Journal of the Royal Statistical Society B1995; 57:289–300. http://www.stat.purdue.edu/~doerge/BIOINFORM.D/FALL06/BenjaminiandYFDR.pdf%5Cnhttp://engr.case.edu/ray_soumya/mlrg/controlling_fdr_benjamini95.pdf.
23. Yum K, Wang ET, Kalsotra A. Myotonic Dystrophy: Disease Repeat Range, Penetrance, Age of Onset, and Relationship Between Repeat Size and Phenotypes. Current Opinion in Genetics & Development2017; 44:30–37. Published online: 2017. DOI: 10.1016/j.gde.2017.01.007. [PubMed: 28213156]
24. Cumming SA, Jimenez-Moreno C, Okkersen K, Wenninger S, Daidj F, Hogarth F, et al.Genetic determinants of disease severity in the myotonic dystrophy type 1 OPTIMISTIC cohort. Neurology2019; 93:e995–e1009. Published online: 2019. DOI: 10.1212/WNL.0000000000008056. [PubMed: 31395669]
25. Radunsky D, Blumenfeld-Katzir T, Volovyk O, Tal A, Barazany D, Tsarfaty G, et al.Analysis of magnetization transfer (MT) influence on quantitative mapping of T2 relaxation time. Magnetic Resonance in Medicine2019; 82:145–158. Published online: 2019. DOI: 10.1002/mrm.27704. [PubMed: 30860287]

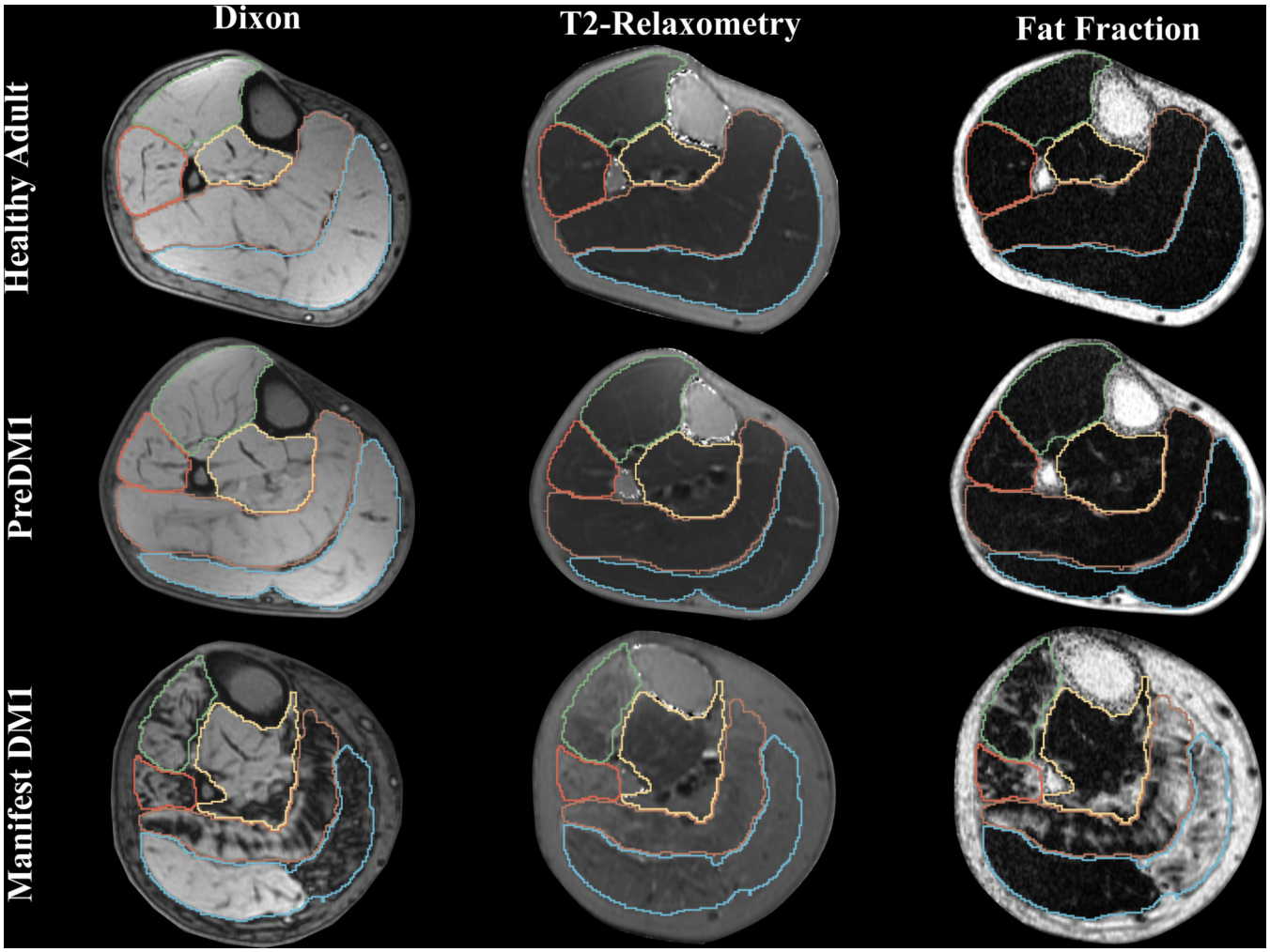

Figure 1. Example images across group and image modality.

Examples of Dixon, T2-relaxometry and FF for similar-aged males from each group. The individual with manifest DM1 had a MIRS score of 4. The green line demarcates TA, orange PL, yellow TP, brown SOL, and blue marks GAS.

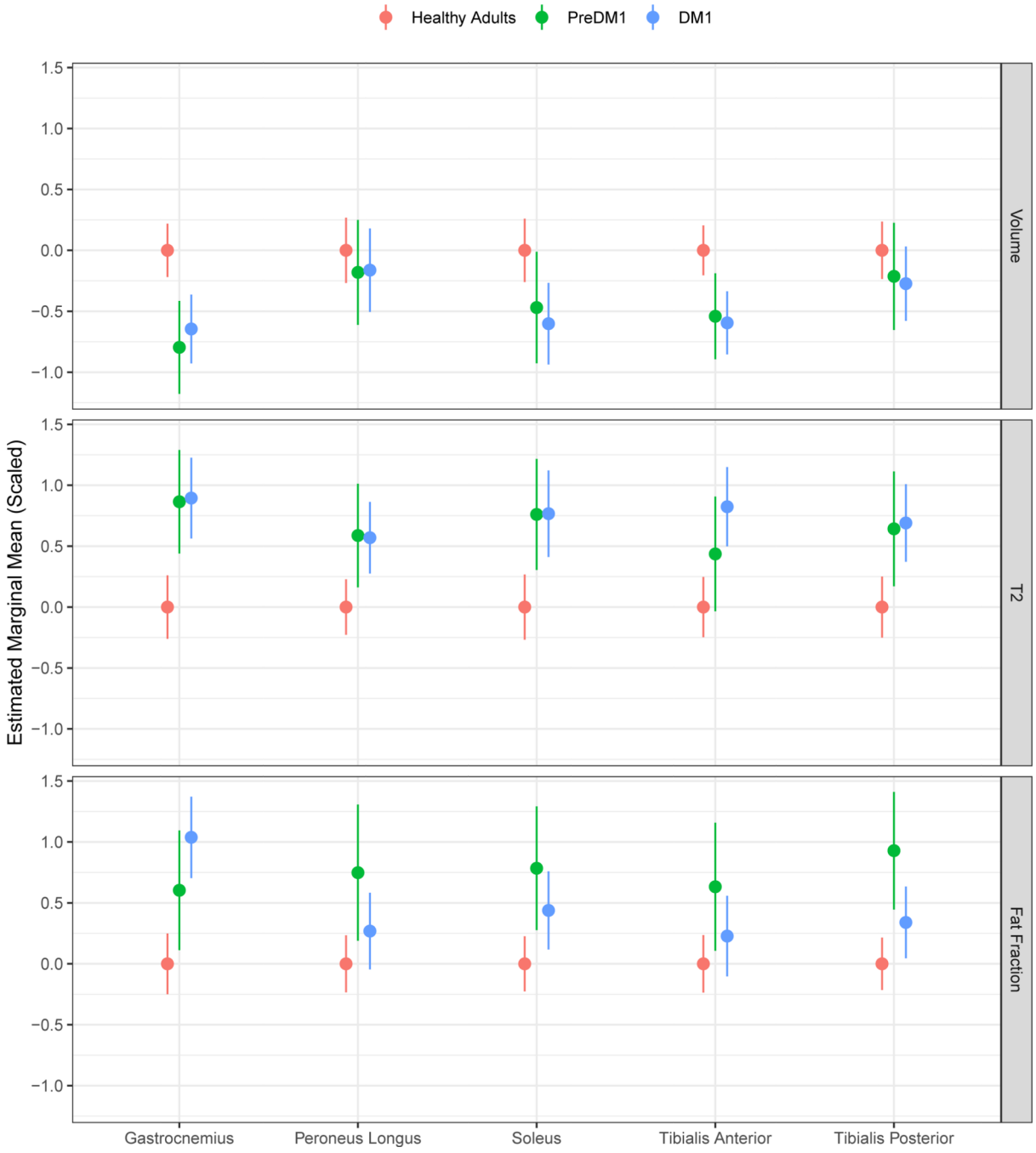

Figure 2. Estimated marginal means for each muscle compartment across image modality.
Estimated marginal means (EMM; adjusted for age, sex, and random effects of family and participant) are shown for healthy adults, PreDM1 and DM1. To convey differences between unaffected and affected individuals, values were centered around the EMM of unaffected individuals. Note that values were scaled to facilitate comparisons across muscles and image modalities.

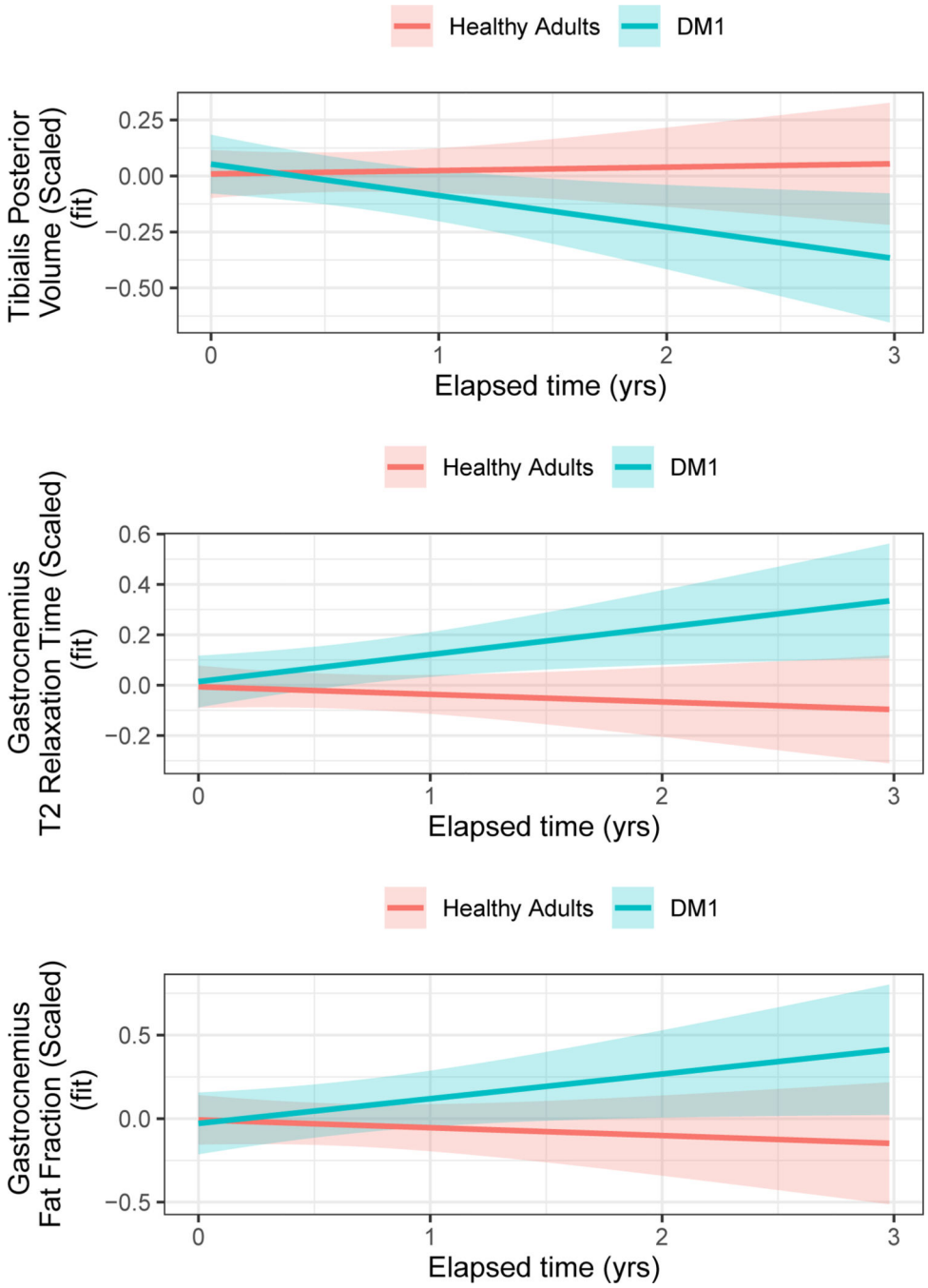

Figure 3. Differences in rates of change across groups.

Group*elapsed time interaction effects were identified for TP volume (top) panel and T2-relaxometry (middle) and FF (bottom) of the GAS. The curves were adjusted for age at baseline, sex and random effects of participants and families. TP volume decreased over time in DM1 patients, while this volume remained stable in unaffected adults (top). GAS T2-relaxation and FF (middle and bottom panels, respectively) showed a significant increase over time in DM1 patients, while these parameters remained stable in unaffected adults.

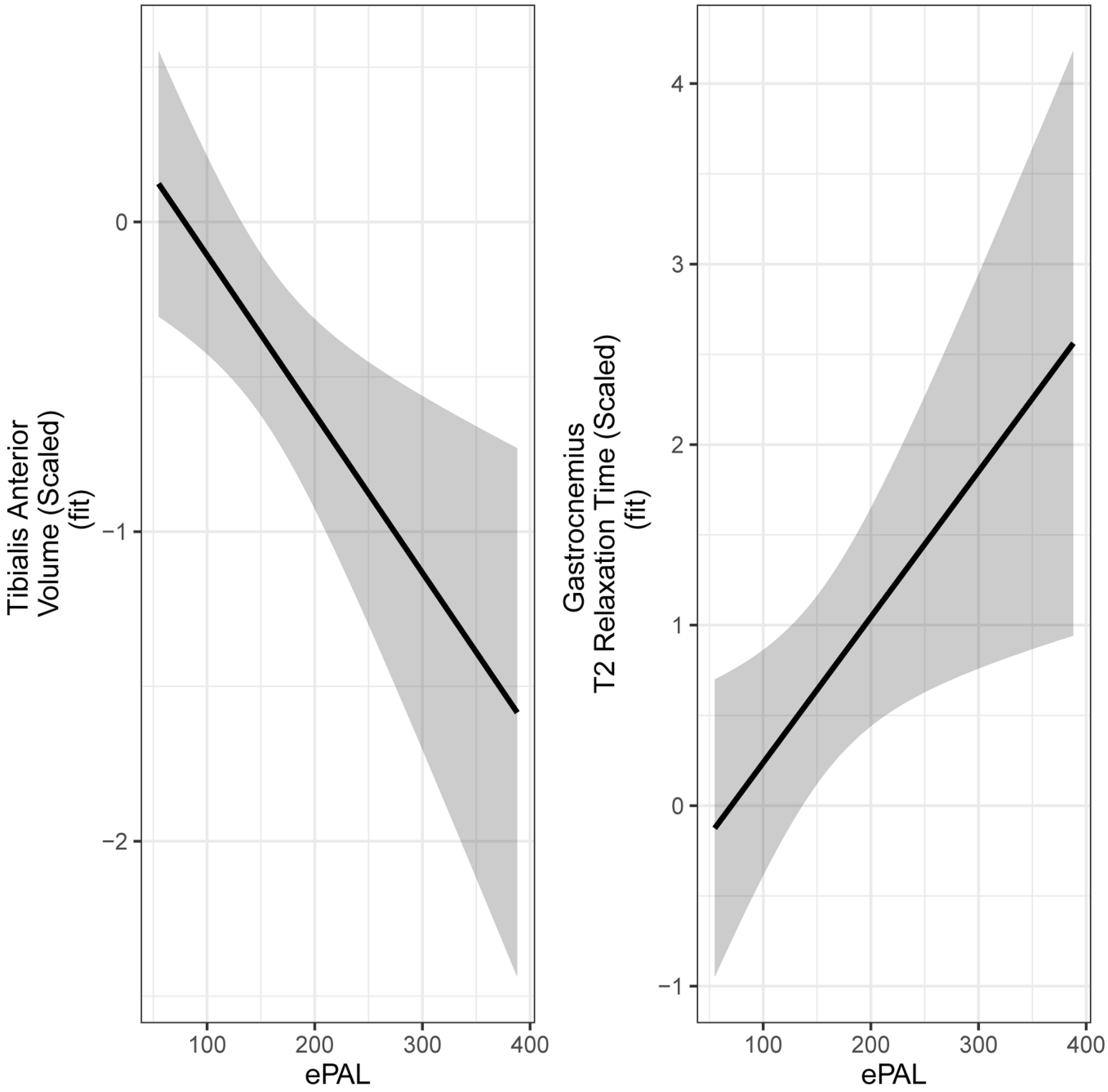

Figure 4. Significant associations between ePAL and muscle MRI

Increased ePAL was associated with reduced volume of the TA volume (left) and increased T2 relaxometry of the GAS (right). The curves were adjusted for age at baseline, sex and random effects of participants and families.

Table 1

Demographics and clinical characteristics, representing number of observations

	Healthy Adults (N=92)	PreDM1 (N=16)	DM1 (N=51)
Sex			
Females	45 (48.9%)	7 (43.8%)	29 (56.9%)
Males	47 (51.1%)	9 (56.2%)	22 (43.1%)
Visit			
1	49 (53.3%)	10 (62.5%)	26 (51.0%)
2	35 (38.0%)	6 (37.5%)	19 (37.3%)
3	8 (8.7%)	0 (0%)	6 (11.8%)
Age (yrs)			
Mean (SD)	42.2 (12.7)	49.3 (16.1)	46.9 (11.0)
Median [Min, Max]	39.7 [18.3, 64.2]	54.6 [22.7, 65.5]	46.8 [20.5, 63.5]
ePAL			
Mean (SD)	14.7 (7.03)	106 (70.3)	158 (77.2)
Median [Min, Max]	13.0 [5.00, 43.0]	84.0 [55.0, 276]	143 [67.0, 388]
Missing	2 (2.2%)	0 (0%)	3 (5.9%)
Muscle Impairment Rating			
No muscle impairment	8 (8.7%)	16 (100%)	0 (0%)
Minimal muscle impairment	0 (0%)	0 (0%)	36 (70.6%)
Distal weakness	0 (0%)	0 (0%)	11 (21.6%)
Mild proximal weakness	0 (0%)	0 (0%)	4 (7.8%)
Severe proximal weakness	0 (0%)	0 (0%)	0 (0%)
Missing	84 (91.3%)	0 (0%)	0 (0%)
Height (cm)			
Mean (SD)	174 (10.7)	171 (8.85)	173 (9.71)
Median [Min, Max]	173 [155, 205]	173 [158, 183]	169 [160, 199]
Missing	1 (1.1%)	0 (0%)	0 (0%)
Weight (kg)			
Mean (SD)	82.8 (14.1)	85.0 (16.9)	72.7 (14.8)
Median [Min, Max]	82.8 [53.2, 131]	83.2 [58.3, 117]	73.2 [50.6, 104]
Missing	1 (1.1%)	0 (0%)	0 (0%)

ePAL could not be determined for 1 individual with DM1 (3 observations); however, this individual had undergone clinical, predictive testing that confirmed presence of DM1. Eight healthy adults underwent clinical MIRS evaluation, because they were enrolled as ‘at risk’, i.e., it was not clear if they had inherited the DM1 mutation at the time of evaluation.

Table 2

Statistics for group*elapsed time interaction across all dependent variables

Modality	Variable	Interaction Statistic*	p	fdr
Volume	Tibialis Anterior	$X^2_{(1)}=0.046$	0.830	0.859
	Tibialis Posterior	$X^2_{(1)}=3.886$	0.049	0.308
	Soleus	$X^2_{(1)}=0.388$	0.534	0.859
	Gastrocnemius	$X^2_{(1)}=2.444$	0.118	0.354
	Peroneus Longus	$X^2_{(1)}=0.724$	0.395	0.846
T2 Relaxation Time	Tibialis Anterior	$X^2_{(1)}=0.533$	0.465	0.859
	Tibialis Posterior	$X^2_{(1)}=0.065$	0.799	0.859
	Soleus	$X^2_{(1)}=1.686$	0.194	0.485
	Gastrocnemius	$X^2_{(1)}=4.844$	0.028	0.308
	Peroneus Longus	$X^2_{(1)}=0.145$	0.704	0.859
Fat Fraction	Tibialis Anterior	$X^2_{(1)}=2.544$	0.111	0.354
	Tibialis Posterior	$X^2_{(1)}=0.050$	0.824	0.859
	Soleus	$X^2_{(1)}=0.031$	0.859	0.859
	Gastrocnemius	$X^2_{(1)}=3.494$	0.062	0.308
	Peroneus Longus	$X^2_{(1)}=0.089$	0.766	0.859

* represents the group*elapsed time interaction in a model that included age at baseline, sex, and random effects for family and participant.

Table 3

Association between ePAL and muscle MRI

Modality	Variable	Coefficient (Std Error	$t_{(df)}$	p	fdr
Volume	Tibialis Anterior	−0.005 (0.002)	$t_{(30.3)}$=−2.961	0.006	0.089
	Tibialis Posterior	−0.002 (0.002)	$t_{(26.6)}$=−0.874	0.390	0.613
	Soleus	−0.002 (0.002)	$t_{(27.5)}$=−0.703	0.488	0.613
	Gastrocnemius	−0.002 (0.002)	$t_{(28.1)}$=−1.195	0.242	0.613
	Peroneus Longus	−0.003 (0.002)	$t_{(28.4)}$=−1.109	0.277	0.613
T2	Tibialis Anterior	0.002 (0.004)	$t_{(25.9)}$=0.635	0.531	0.613
	Tibialis Posterior	0.004 (0.003)	$t_{(28.3)}$=1.257	0.219	0.613
	Soleus	0.002 (0.004)	$t_{(30.1)}$=0.641	0.526	0.613
	Gastrocnemius	0.008 (0.003)	$t_{(30.1)}$=2.474	0.019	0.144
	Peroneus Longus	0.003 (0.003)	$t_{(21.8)}$=0.957	0.349	0.613
Fat Fraction	Tibialis Anterior	0.002 (0.003)	$t_{(32.5)}$=0.876	0.388	0.613
	Tibialis Posterior	−0.0005 (0.003)	$t_{(29.9)}$=−0.182	0.857	0.857
	Soleus	0.002 (0.003)	$t_{(28.7)}$=0.694	0.493	0.613
	Gastrocnemius	0.005 (0.004)	$t_{(21.4)}$=1.288	0.211	0.613
	Peroneus Longus	0.0007 (0.003)	$t_{(38.3)}$=0.288	0.775	0.830

Abbreviations: Std.Error=standard error; t(df)=t-statistic (degrees of freedom); *p*=p-value; and *fdr*=false discovery rate.

The coefficient refers to the coefficient for ePAL.